Hindawi Publishing Corporation

Science and Technology of Nuclear Installations
Volume 2008 (2008), Article ID 874969, 14 pages
doi:10.1155/2008/874969

Project Report

Natural Circulation Characteristics at Lo

Conditions through PANDA Experiments

Domenico Paladino,[1] Max Huggenberger,[1] and Frank Schäfer[2]

[1]Laboratory for Thermal-Hydraulics, Paul Scherrer Institute (PSI),
[2]Research Center Dresden-Rossendorf, P.O. Box 510119, 01314 D

Received 31 July 2007; Accepted 2 January 2008

Academic Editor: John Cleveland

Abstract

Natural circulation characteristics at low pressure/low power
investigations and numerical simulations. The PANDA large-scale
data on natural circulation characteristics as a function of sever
conditions. The new experimental data allow for testing and in
computer codes to be used for treating natural circulation loops
presents a synthesis of a part of the results obtained within the EU
performance of boiling water reactors." It does so by using the
showing some examples of numerical simulations performed with t

1. Introduction

In the framework of the EU-Project NACUSP, experiments on the cooled boiling water reactors (BWR) have been performed in four complement each other, ranging from small-scale to large-sca conditions to the nominal operating conditions for BWRs. The economics of operating and future plants through improved (increased confidence levels on the safety margins regarding the sta

This paper presents a synthesis of the results obtained from the facility [2] and from the numerical simulations performed with t parameters covers a large spectrum of conditions for the low-pres especially with regard to the start-up procedures for natural- simplified boiling water reactor (ESBWR)).

2. PANDA Experimental Investigations

2.1. PANDA Facility

The multipurpose thermal-hydraulic test facility PANDA is loc Switzerland. The facility is designed and used for investigating a different light water reactor (LWR) designs. PANDA has a modular vessels with a total volume of 460 m^3 and four open pools with a pressure vessels are arranged in two vertical columns. The two lo chamber are interconnected with two large pipes. The wetwell vess They are interconnected at about midplane elevation with one larg (GDCS) pool. The sixth vessel is configured to simulate the react performing natural circulation tests at roughly 1 : 1 scale in height is 19.2 m in height. The RPV includes a heated section, a riser, height of 1.3 m and does not reproduce the geometry of a real co elements divided into six individually controlled groups. This allow to 1.5 MW. The heaters are distributed over the cross-section to power range. The riser has a height of 9.5 m (starting at the top are placed on top of the drywell vessels and are equipped with insulated in order to minimize heat losses: an insulation layer of system lines and pools. The overall height of the facility is about bar and 200 °C.

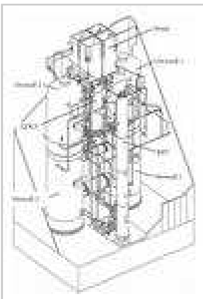

Figure 1: PANDA facility.

The basic instrumentation of the facility includes about 1000 sens differences, water levels, flow rates, gas concentrations, fluid acquisition system maximum scanning rate is 5 Hz. The standar remotely controlled from a graphical-display man-machine interfac

2.1.1. PANDA Facility Configuration for Natural Circulation T

For the NACUSP project only parts of the PANDA facility were used the RPV natural circulation loop and the condensation/cooling lo condenser and condenses due to the temperature difference w temperature). The pool is open to the atmosphere and water evap through the drain line back to the RPV downcomer. A major mo region. A movable ring was attached to the lower edge of the sh allow for varying the core-inlet hydraulic resistance. The gap he bottom of the RPV can be varied in order to obtain the require systems are used for preconditioning the facility and for adding wa test duration.

Figure 2: PANDA configuration for natural circ

The instrumentation in the RPV has been significantly improved. I circulation tests. Additional K-type thermocouples inside riser and fluid and wall temperatures. In the range of 100 $^\circ$C – 150 $^\circ$C a me For higher temperatures the error is still less than 1 $^\circ$C. Three ul local fluid flow velocities in the downcomer. The measurement er reading. Absolute pressure and heater power are measured as w downcomer allow for the assessment of void fraction in differe reflectometry (TDR) probe is used to measure the level swelling du

2.2. PANDA Test Matrix

The test matrix allowed the RPV power and pressure to be varied, circulation behavior such as core-inlet hydraulic resistance and RPV power, balanced by a corresponding condenser heat removal ca match the desired steady state pressure in the RPV. The basic pressure level, the maximum energy is removed if the condenser power for the four specified pressure levels is given in Table 1 (c the condenser heat removal capacity is adjusted by lowering the w condenser area. Three tests with different power (“low,” “midc four different pressure levels.

Table 1: Basic test matrix (variation of pressu

The core-inlet hydraulic resistance coefficient *k* has been varied a was used $(k_{\text{basic}} = 30)$. Selected tests were performed with a l resistance $(k_{\text{high}} = 500)$.

The RPV water level has also been varied: most of the tests were p above bottom of RPV. This level represents about the nominal valu reduced close to top of riser which is at 11.0 m above RPV bottom

The following three series of tests with totally 25 experiments have

(i) B-series tests (BWR-typical core-inlet flow resistance $k =$

(a) 12 tests with nominal RPV water level (12.8 m),
(b) 2 tests with low RPV water level (11.1 m and 11.4

(ii) L-series tests (Low core-inlet flow resistance $k = 7$):

(a) 3 tests with nominal RPV water level (12.8 m),
(b) 1 test with low RPV water level (11.1 m);

(iii) H-series tests (High core-inlet flow resistance $k = 500$):

(a) 6 tests with nominal RPV water level (12.8 m),
(b) 1 test with low RPV water level (11.1 m).

An overview of all PANDA tests is included in Table 2.

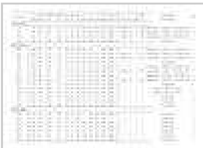

Table 2: Overview of the PANDA tests and ana

2.3. Experimental Results and Analysis

Natural Circulation Modes

The coolant temperature increases in the heated section (core), b given conditions. A rough estimation of the position of the boiling was performed. The temperature measured at the inlet of the cor coarsest assumptions were made (no heat losses, uniform radial subcooled boiling). The nondimensional value $z^*_{\text{boil},b}$ reported in T the inlet of the core, and divided by the length of the core) $z^*_{\text{boil},b} \leq 1$: boiling in the core; $z^*_{\text{boil},b} > 1$: no boiling in the core). T any test except may be in tests with high core-inlet resistance and

In the same way, a coarse estimation of the height in the riser at made. Using the same inlet temperature, calculating the temper conserved all along the riser (no heat losses), a distance z^*_{flash} (me riser) is estimated and reported in Table 2. For most of the tests, upper region or above the riser. Of course, in tests at high core-in tests with low RPV water level (and hence lower pressure head sections of the riser.

These estimations do not take into account the 3D and local effect flow regime actually occurring in the RPV. Some interesting info temperature profiles measured in the central axis of the RPV. Two corresponding to the saturation temperature is also plotted on e estimated by using the time-averaged RPV pressure and calcul considering the possible presence of void.

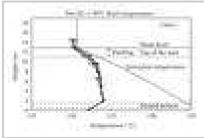

Figure 3: Measured temperature profiles in th

From Figure 3, it is clear that the validity of the comparison with the error in temperature measurements. Due to the data redu temperature (Figure 3). The saturation temperature decreases alc pressure. Flashing should occur when the coolant reaches saturati in test H2.1 (shown in Figure 3(a)), the average height of the fla about the level corresponding to the top of the riser. In this case, profile above this height, where measured temperatures seem t basically confirms the previous coarse prediction (Table 2, z^*_{flash} = (Figure 3(b)): the fluid temperature clearly following the saturatic occurred along the complete riser length. To summarize, these diff cases and define three classes:

Class 1. flashing above the riser, or perhaps no flashing at all (Figu

Class 2. flashing at a lower elevation in the riser;

Class 3. two-phase flow all along the riser (Figure 3(b)). Rough processed from differential pressure measurements also indicate top of the riser, and especially for cases with high core-inlet resist largest difference between the swell level (measured by the TDR p differential pressure measurements. For example, in tests HL5.3 estimated in the upper region of the riser. In the lower sections, va

Analysis of Flow Velocity Measurements in RPV Downcomer

The natural circulation flow rate is of main interest. Hence, this s from 3 ultrasonic flow meters in the RPV DC. The sensors are locat angle of 120° azimuthally between each other.

The velocity signals were sampled at a frequency of 0.5 Hz for th noted that the time constant of the sensors was set to 6 seconds spectral density (APSD) of the signals was calculated to ider autocorrelation function (ACF) was used to calculate the decay r parameter to quantify the stability of the system: if $\text{DR} < 1$, the sy practice, the DR values presented in Table 2 were estimated by s the first maxima of the ACF (Figure 4(c)). Cross-power spectral d were also calculated to examine coherence, possible phase shifts meters.

An overview of the results of the analysis performed can be found given in the first columns of this table. Mean values of the veloci are also reported. V_{123} is the average of the three mean velocitie the intensity of the velocity fluctuations, and was calculated as foll

$$I_{123}(\%) = 100.\frac{(\text{Var}_{12}}{V_1}$$

where Var_{123} represents the average of the 3 variances of the si
result in very high values for the tests with very low natural circula
expected to be higher (e.g., test H2.3).

Concerning the spectral analysis, the frequency and the correspo
possible. The value "0" in the column "$\Delta\varphi$" of Table 2 means
was observed, that is, the three velocity signals were oscillating i
DR was estimated from the ACF and is also reported in Table 2.
signals from the sensor measuring the total pressure in the I
characterize some of the tests. Looking at the spectra and at the
estimation of DR values, the PANDA tests can be categorized in tw

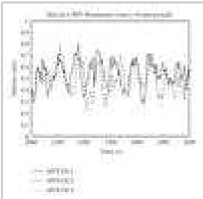

Figure 4: Analysis of flow velocity signals in th

1st Group

The rows in Table 2 corresponding to these tests are greyed. A
results. An excerpt of the raw velocity signals recorded during this
observed on the processed spectra of the 3 sensors reported in F
show that the three sensors oscillate "together," that is, with r
was confirmed by looking at the phase of the complex cross-pow
Just simply looking at a number of raw signals recorded over th
measured variables (temperatures, pressure in the RPV, condense
the same frequency. The ACF obtained from velocity signal 1 is g
stable behavior ($DR = 0.64$) can be estimated from this graph.

2nd Group

An illustration of this group is given using test B3.3 results. Obse
this case show rather *random* behavior. In some other tests belon
observe significant phase shifts between the sensors. Figure 5(b) s
in the power spectrum. Using a logarithmic scale, the low-frequ
Moreover, the ACF does not really allow a DR value to be derived (
(actually, very close to 0) compared to the tests of the first group.

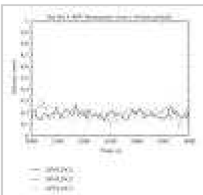

Figure 5: Analysis of flow velocity signals in th

It was also observed that these two characteristic modes of beha
function of time during the course of the tests. For tests L8.3 ar
successive (1-hour long) time periods and it clearly showed that,
times were very similar.

Some data from other sensors (condenser feed and drain flow ra
using the same approach as for the velocity data. For the tests fro
at the same oscillation frequency. No peak can be found for the te
of these tests (e.g., test B3.3), the condenser feed flow and R
spectrum whereas no such peak was observed for the velocity si
concerning the analysis of RPV pressure signals). This indicates tha
riser, not influencing the main circulation flow. These cases fall cor

From the expected mechanism of the flow oscillations, the fluid tr
time of the enthalpy perturbations in the adiabatic section, sho
oscillations. From Figure 11, it is clear that the oscillation period
total transit time can be evaluated as the sum of the transit time
the heated section [3]. In PANDA, no velocity measurement is ava
was made by simply using the time-averaged value of the velocity
the flow area ratio between the riser and the DC.

Following this simplified approach, the oscillation period was found
the fluid (Figure 6). The simple way in which the transit time was
phase flow in the riser. Hence, it is likely that our assessment over
to be quite consistent with those presented for the CIRCUS facility
be twice the transit time.

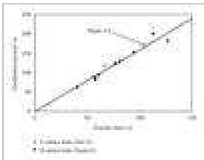

Figure 6: Period of oscillation versus fluid tran

Discussion

The differentiation between the two groups of tests is based on DR
the validity and the accuracy of this method can be questioned
stability parameters and can be compared to the ACF-based me
velocity time traces were processed using a more sophisticated
method properly applied to our signals yielded about the same DR
the main result from this analysis that all tests are stable.

However, by having a closer look to the tests, the different flow re
defined, can be related to the previous findings regarding the stab
was used for this purpose. The plots in Figure 3 partly illustrate the

Class 4 (Figure 3(a)). High inlet subcooling and relatively low (or
is likely that flashing occurred only above the riser, the natural c
This would explain why, in some of these tests, contrary to the ve
show a peak in their spectrum and allow the derivation of DR valu
some of these tests (notably those performed at the lowest powers

Class 5. These tests, performed at relatively high power and low
identified oscillation period and DR values could be derived from
flow rates were measured in these tests, which indicate the co
production and of a low inlet resistance. According to our estima
but flashing did in the upper half of the riser.

Class 6 (Figure 3(b)). Very stable behavior was found for these t
Under these conditions, the flashing front fluctuates close to the t
two-phase natural circulation. The measured flow rates are among
flow resistance. Looking at the parameters (notably the expected p
and at the characteristic temperature profiles (Figure 3(b)), it se
can be assumed in these cases.

The presented classification gives a rather coherent picture of t
experimental observations with the expected phenomenology.
characterization of the tests (from single-phase to two-phase flow
what is reported in the literature. Test BLL5.3, which shows a D
conditions.

The test matrix allowed the variation of the RPV water level. How
flow behavior cannot be clearly assessed. Comparing tests B5.3 a
stabilizing effect.

3. ATHLET Simulations

3.1. Thermal-Hydraulic Model

The thermal-hydraulic code ATHLET [4], which has been dev
Reaktorsicherheit mbH), was used for the calculation of selecte
Section 2). The ATHLET input dataset models all main parts of the
circulation experiments (Figure 7).

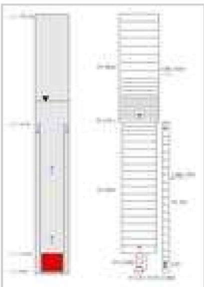

Figure 7: Schematic representation (a) and A

The ATHLET model consists of the lower plenum (P1-LP-1), the
elements, the riser (P1-RIS1), upper plenum (P1-UP-1), downco
RIS2). The isolation condenser (IC) is not modeled. Therefore, a
upper part of the RPV and to the downcomer, modeling the IC-fe
and given enthalpy (only drain line). In all control volumes, the 5
for liquid and vapour mass and energy, mixture momentum equa
are used. A valve at the lower end of the downcomer (VLV, see F
core inlet. The cross-section of this valve can be changed to adjust

3.2. Steady State Calculation

At first, a steady state calculation with constant boundary conditio
these calculations, the pressure losses, heat losses, the RPV wa
adjusted. The steady state calculation starts with zero power. Afte
the power is increased with time. For the calculations, it was not
inlet, because the form-loss coefficients are changed within the alg

calculation. Therefore, a valve at the lower end of the downcomer core-inlet flow resistance. The cross-section of this valve was i corresponding to the measured data. The steady state calculation example, the results of the steady state calculation for Test B 8.3 a in Figure 8.

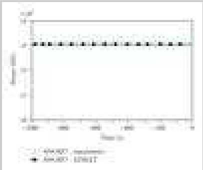

Figure 8: Core power (MW.RP.7), system downcomer velocity (MVE.DC.1) for test B 8.3:

3.3. Transient Calculations

From the PANDA test matrix, 5 experiments were selected for t conditions calculated with ATHLET in comparison to the measured over a period of 5 hours. The experimental data in Table 3 repre ATHLET simulations correspond to the end of the steady state calcu

Table 3: Initial conditions for the selected P Calculation, Add. Calc. = Additional ATHLET ca

Each transient calculation starts from a steady state calculation a behavior with respect to natural circulation stability a short disturb to stimulate oscillations in the loop (see Figure 9). The response mass flow.

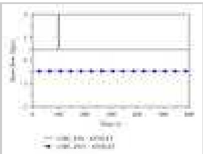

Figure 9: Mass flow in IC-feed and drain line RIS1).

As in the experiments, the DC velocities were used to calculate t the downcomer velocity, the spectrum, and the autocorrelation fu Test B 3.3). Both calculations predict stable behavior and no lin drain line mass flow leads to flow oscillations with decreasing amp due to the higher core-inlet loss coefficient ($k = 30$) used in the B damped in the ATHLET simulations, an oscillation period and also flow. Table 4 gives a comparison between measured and calculat tests.

Table 4: Oscillation period and decay ratio experiment, Cal. = ATHLET calculation).

Figure 10: DC velocity, spectrum, and autoc tests B 8.3 and B 3.3.

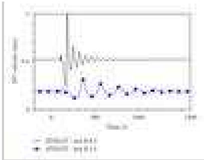

Figure 11: Oscillation period as a function (ATHLET simulations.

The experiments and also the ATHLET calculations show that th velocity. This behavior is illustrated in Figure 11. The results of th the experimental data.

To demonstrate the ability of ATHLET to calculate an unstable calculation with a core-inlet loss coefficient of $k=7$, a higher core initial conditions for this calculation are given in Table 3. The resul strong oscillations caused by flashing in the riser section. Figure 12 and the autocorrelation function. The oscillations have a period of (

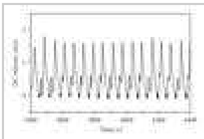

Figure 12: DC velocity, spectrum, and aut calculation with higher core power and lower R

In Figure 13, the calculated temperature distribution over the he seconds. At this time, the dynamic behavior becomes unstable. production takes place. Only above the middle of the riser section, flashing-induced oscillations occur.

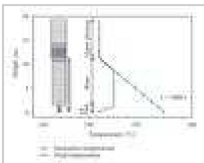

Figure 13: Temperature distribution over the calculation).

4. Conclusions

In the PANDA facility, 25 tests have been carried out in order t stability, under low-pressure/low-power conditions. Some param varied, such as the RPV power and pressure, the core-inlet hydraul

An analysis of the data from three ultrasonic sensors installed at was presented. The power spectra show, in a few tests, a major a of the flow rate seems to be of the order of twice the transit time show that these cases are stable. The tests for which more flat s more stable.

A phenomenological classification has been applied according to single-phase circulation (with possibly flashing above the riser), t of the riser, or two-phase flow along the complete riser length. Th natural circulation flow under low-pressure conditions represent notably because the height of the riser in PANDA is approximately have been used for assessing the capabilities and limitations circulation characteristics at low pressure/low power.

The ATHLET simulations show stable behavior for the selected PA damped and no limit-cycle oscillations occur. The calculated period experimental results. With help of the additional calculation, it cou an unstable behavior. In this case, strong oscillations occur, cause

Acknowledgment

This work was supported by the European Commission (EU 5t NACUSP Project) and by the Swiss Federal Office for Education and

References

1. C. Aguirre, D. Caruge, F. Castrillo, et al., "Natural circulatic *Nuclear Engineering and Design*, vol. 235, no. 2–4, pp. 401
2. O. Auban, D. Paladino, and R. Zboray, "Experimental inves low-power/low-pressure conditions in the large-scale PANDA 294–312, 2004.
3. A. Manera and T. H. J. J. van der Hagen, "Stability of natur start-up: experimental results," *Nuclear Technology*, vol. 1
4. G. Lerchl and H. Austregesilo, "ATHLET Mod 1.2 Cycle B: U